



Antibacterial, Antifungal Chalcone Derivatives as EGFR Inhibitors-Molecular Docking and ADMET Studies

Hemalatha Sattu^{1*}, Indira rani Nerella¹ and Saritha Jyostna Tangeda¹

¹Department of Pharmaceutical Chemistry, Sarojini Naidu Vanitha Pharmacy Maha Vidyalaya, Tarnaka, Secunderabad-17, Telangana, India.

Authors' contributions

This work was carried out in collaboration among all authors. All authors read and approved the final manuscript.

Article Information

DOI: 10.9734/JPRI/2021/v33i45B32819

Editor(s):

(1) Dr. Amal Hegazi Ahmed Elrefaei, Hot Lab and Waste Management Center, Egypt.

Reviewers:

(1) Arpita Yadav, CSJMU Kanpur, India.

(2) Biswajit Dash, NEPEDS College of Pharmaceutical Sciences, India.

Complete Peer review History: <https://www.sdiarticle4.com/review-history/74657>

Short Research Article

Received 28 July 2021

Accepted 03 October 2021

Published 08 October 2021

ABSTRACT

Aim: In our earlier research, we have synthesized series of substituted 1-(2, 5-dimethyl thiophene-3yl)-(4-substituted phenyl)-2-propene-1-one derivatives and evaluated them for their anti-bacterial and antifungal activity. In recent years, chalcone derivatives are proved for their varied pharmacological effects ranging from antimicrobial activity to anti-cancer effects. In this study, we have hypothesized the efficiency of our earlier synthesized anti-bacterial and antifungal chalcone derivatives for their potential inhibition of epidermal growth factor receptor protein (EGFR), through molecular docking studies.

Methodology: Molecular docking simulation studies are performed using the Glide XP module of Schrodinger Suite and ligand binding energies are also calculated.

Results: Molecular docking studies of the selected compounds against EGFR revealed docking scores ranging from -6.746 (compound 5) to -5.681 (compound 3) and also provided insight into binding conformations of the ligands in the EGFR protein environment. Additionally, molecular property and Absorption, Distribution, Metabolism, and Excretion (ADME) predictor analysis is also performed for the dataset ligands, which further provided the probable explanation for the binding potentials.

*Corresponding author: E-mail: hemalathasattu0@gmail.com;

Conclusion: Among all the tested dataset ligands, compound 5 has shown the highest dock score (-6.746) with better ADME profiles. Binding energies in the protein-ligand interactions explain how fit the ligand binds with the target protein. Molecular docking studies of these anti-bacterial, antifungal chalcone derivatives provided deeper insights in understanding the probable conformations of these tested ligands in the EGFR protein environment.

Keywords: EGFR; chalcones; molecular docking; binding energy; ADME.

1. INTRODUCTION

Chalcones, two aromatic rings are linked by an aliphatic three-carbon chain with conjugated double bonds [1] in which derivatization mainly occurs through the substitutions on the aromatic rings resulting in a distinct variety of compounds. Chalcones possess distinct variety of pharmacological activities like anti-bacterial [2], anti-fungal [3], anti-inflammatory [4], anti-oxidant [5], anti-tuberculosis [6], anti-malarial [7], analgesic [8], anti-HIV [9], anti-tumor [10].

These chalcone derivatives exhibited anticancer activity on various drug-sensitive cell lines [11]. In silico studies on chalcones revealed that they have interaction with various cellular proteins which are responsible for causing cancer like CDK7, EGFR, etc. During these years chalcones proved to be potent against the EGFR group of proteins.

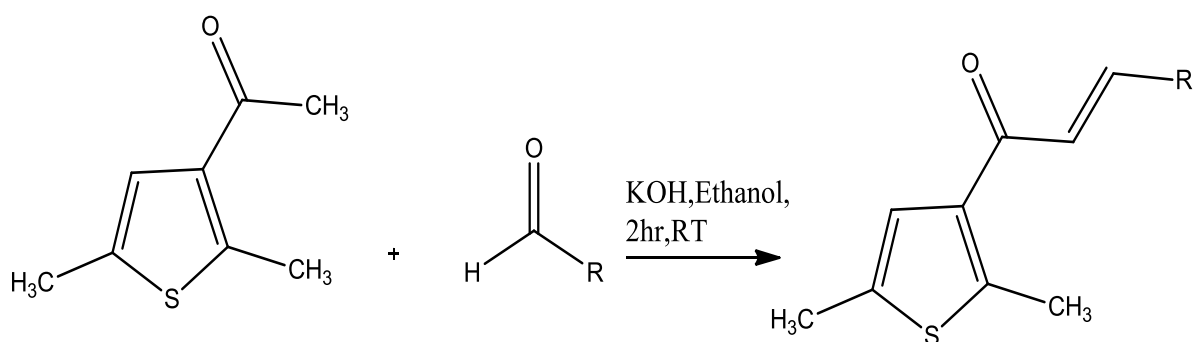
In the present investigation, we have hypothesized the inhibitory potentials of the anti-bacterial, anti-fungal chalcone derivatives which were earlier designed and developed in our laboratory against EGFR protein [12]. To

evaluate our hypothesis we have performed molecular docking studies to the data set compounds along with calculation of ligand binding energies. Additionally, we have also performed predictor analysis of molecular properties and ADME scores of the data set ligands.

2. MATERIALS AND METHODS

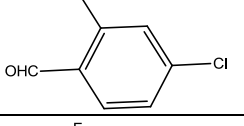
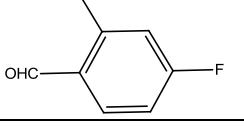
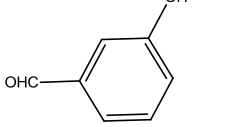
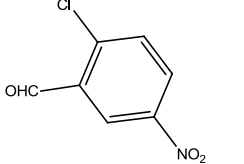
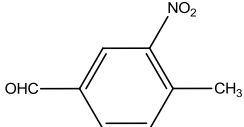
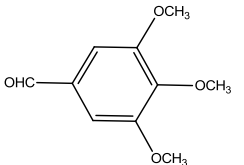
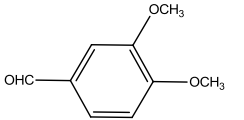
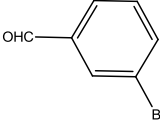
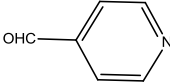
2.1 Dataset Ligands and Ligand Optimization

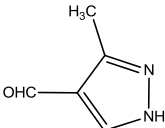
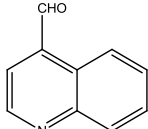
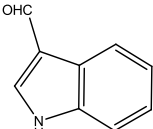
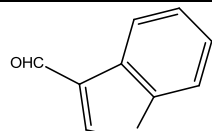
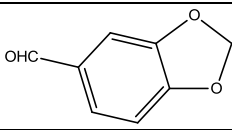
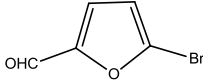
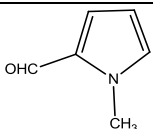
Anti-bacterial, anti-fungal activity possessing chalcone derivatives which were earlier developed in our laboratory was selected (Scheme 1) [2]. 2D structures of the compounds were converted to 3D using potential algorithms and application of high efficient force fields. Initial geometrical optimization and energy minimization of molecules was performed by using the Ligprep tool of Schrodinger suite [13]. Various ionization states were generated using the Ligprep module using a special program EPIK along with various possible conformers and tautomers.



R-2-chloro phenyl, 4-fluoro phenyl, 2,4-difluoro phenyl, 4-nitro phenyl, 3-hydroxy phenyl, 4-methylphenyl, 2-chloro5-nitro phenyl, 3-nitro4-methyl phenyl, 3,4,5-trimethoxy phenyl, 3,4,-dimethoxy phenyl, 4-pyridyl, 1-phenyl 3-methyl pyrazol, 3-quinazoline, 4-imidazole, 3-indole, piperanol, 5-bromo2-furfural, n-methyl2-pyrrole

Scheme 1. Synthesis of chalcone derivatives

Compound	R
1	
2	
3.	
4.	
5.	
6.	
7.	
8.	
9.	
10	
11.	
12.	
13.	

14.	
15	
16.	
17.	
18.	
19.	
20.	

The molecular properties of the processed ligands were studied by using the Qikprop module. Qikprop module also predicts ADME profiles like blockage of Human Ether-a-go-go-related Gene (hERG) K⁺ channels, apparent Caco-2 cell permeability, brain/blood partition coefficient, apparent Madin-Darby canine kidney (MDCK) cell permeability, skin permeability, binding to human serum albumin, and human oral absorption of the given set of ligands [14].

2.2 Molecular Docking Studies

The digital structure of the EGFR protein was retrieved from the Protein databank website with PDB Id: 1M17 and the structure was optimized by deleting unbound water molecules which are over 1 Å, adding hydrogen atoms to satisfy the valences, adding missing amino acids to stabilize side chains and energy of the whole structure was minimized using OPLS-2005 force field using Protein Preparation Wizard tool of Schrodinger Suite [15].

Optimized protein structure was used to examine protein-ligand interactions of the dataset ligands

using the Glide Xp docking protocol. Initially, a 3D grid was established to the binding pocket (active site) of the protein, into which all the dataset ligands were docked. Binding interactions and efficiency of the binding were calculated in terms of Glide Score, which is a combination of hydrophilic, hydrophobic, metal-binding groups, Van der Waals energy, freezing rotatable bonds, and polar interactions with receptor [16,17].

$GS_{score} = 0.065 \times \text{Van der Waals energy} + 0.130 \times \text{Coulomb energy} + \text{Lipophilic term (Hydrophobic interactions)} + \text{H bonding} + \text{Metal binding} + \text{BuryP (Penalty for buried polar groups)} + \text{RotB (Penalty for freezing rotatable bonds)} + \text{Site (Polar interactions in the active site)}$

2.3 Post Docking Calculations

Prime MM/GBSA (molecular mechanics-based generalized Born/surface area) module of Schrodinger suite was used to calculate the binding energies of the docked complexes, which is a combination of OPLS molecular mechanics energies (EMM), an SGB solvation model for

polar solvation (GSGB), and a non-polar solvation term (GNP) containing non-polar solvent accessible surface area and Vander Waals interactions. In this, docking results were rescored through an energy function with a well-defined description of binding contributions. The total free energy of binding is then expressed in the form below mentioned Equation [16].

$$\Delta G_{\text{bind}} = G_{\text{complex}} - (G_{\text{protein}} + G_{\text{ligand}})$$

Where ΔG_{bind} is ligand binding energy.

3. RESULTS AND DISCUSSION

3.1 Predicted Molecular Properties and ADME Profile

Various molecular properties such as Molecular weight, dipole, volume, Solvent Accessible Surface Area (SASA), the hydrophobic component of SASA (FOSA), hydrophilic component of SASA (FISA), π (carbon and attached hydrogen) component of the SASA (PISA), and a weakly polar component of the SASA (halogens, P, and S) (WPSA) have been determined using Qikprop module (Table 1). The molecular weight of all the compounds is within the normal range of 135-700 Da. Parameters such as dipole, SASA, FOSA, FISA, WPSA, and volume are also within the normal range for all the compounds. As the predicted molecular properties like SASA, FOSA, FISA, PISA are within the normal range indicates that the Compounds have large surface area with hydrophilic component and decreased hydrophobic component that is in the range of below 200 for maximum set of compounds indicates the decreased probability of crossing blood brain barrier. Predicted dipole moment of all the compounds got 0 instead of normal range indicates that the compound might be planar in nature as both the bonds rotated equally and net dipole moment we got 0.

Predicted ADME parameters include partition coefficient, predicted aqueous solubility (QPlogS), probability of CNS effects, blockage of HERG K⁺ channels (QPlogHERG), apparent Caco-2 cell permeability (QPpCaco), brain/blood partition coefficient (QPlogBB), apparent MDCK cell permeability (QPpMDCK), skin permeability (QPlogKp), binding to human serum albumin (QPlogKhsa) and human oral absorption of the given set of ligands (Table 2). All the compounds possessed higher human oral absorption levels (94%-100%). All the compounds resulted in low to inactive effects towards CNS. The partition

coefficient of all the compounds was within the recommended range (-2.0-6.5), whereas, all the compounds were found to have predicted water solubility in the recommended range. All the compounds were reported to have extremely good apparent Caco-2 cell permeability (> 500) except the compounds 1 and 8 have shown little less apparent Caco-2 cell permeability (<500), and with moderate potential to cross through the blood-brain-barrier (-0.981-0.009). As the predicted ADME properties like blood brain partition coefficient, CNS, human oral absorption are within the normal range indicates these compounds are not crossing the blood brain barrier and does not have any impact on the central nervous system. All these compounds have good oral absorption that is most of the compounds have 100% oral absorption which is a good sign of the compounds.

3.2 Molecular Docking and Binding Energy Calculations

Molecular docking studies were performed to find the possible protein-ligand interactions of the dataset ligands which were earlier proved to have anti-bacterial and anti-fungal activity. Additionally, these also assisted in identifying the conformational changes of the ligand in the protein environment. 100 different protein-ligand complex conformations for each docked complex were generated through the Glide XP module. Based on the EModel energy, only one was displayed in the result. Glide dock scores of the dataset ligands were shown in Table 3 along with the interaction amino acids and number of amino acids. Among the docked ligands, compound 5 reported the highest dock score of -6.746 with EModel energy of -34.578 Kcal/mol. Compound 5 possessed 1 hydrogen bond, with Methionine 769 amino acid at a bond distance of 1.78 Å (Figs. 1 and 2). Dock scores of all the compounds ranged from -6.746 (compound 5) to -5.681 (compound 3). Methionine 769 is the most commonly interacted amino acid with the data set ligands. Other amino acids include Lysine 721 (compound 8, 9, 10, 11), Aspartate 831 (compound 7), and threonine 830 (compound 14). These constitute the kinase domain of EGFR protein. The binding efficiency of compound 20 s is majorly contributed by hydrophobic and other Van Der Waals forces but not hydrogen bonding.

Multi-Ligand Bimolecular Association with Energetics (MBAE) consists of an automated mechanism that calculates the free energy of

binding (FEB) of each docked complex. The total free energy of binding (binding energy) of each ligand is tabulated in Table 3. The total free energy of binding is the difference energy of the complex and ligand & protein which includes solvation energy, Vander wall's energy, electrostatic energy, valence energy, and constraint energy. The compound with the highest dock score (compound 5) possessed the highest binding energy of -34.578 Kcal/mol, whereas compound 7 reported the highest binding energy of -38.845 Kcal/mol compound 3 reported the lowest binding energy of -30.988Kcal/mol. As the synthesized compounds have good dock score and binding nature of

molecule in the protein environment, the hydrophilic nature of the compound plays a major role which is helpful in designing the molecules for further studies like biological activities, pharmacokinetic profile of the molecules etc.

Based on the good dock score the SAR of the compound 5 might be the replacement of one of the phenyl moiety with 2,5 disubstituted thiazole heterocycle might be the reason for enhanced dock score, the two substitutions might be electron donors to the ring. The substitution of chlorine/ atom at 2,4 substitution on another phenyl moiety might be the reason for enhanced dock score.

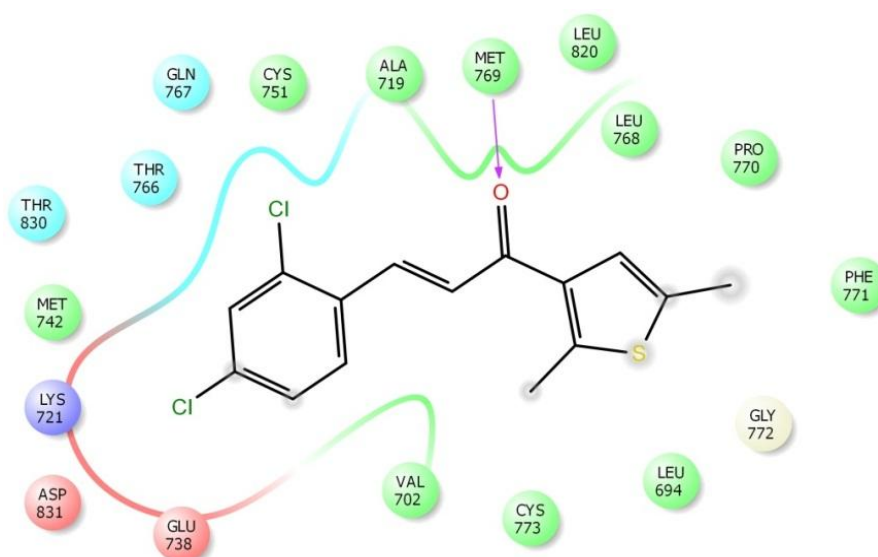


Fig. 1. Binding interactions of compound 5 at kinase domain of EGFR protein

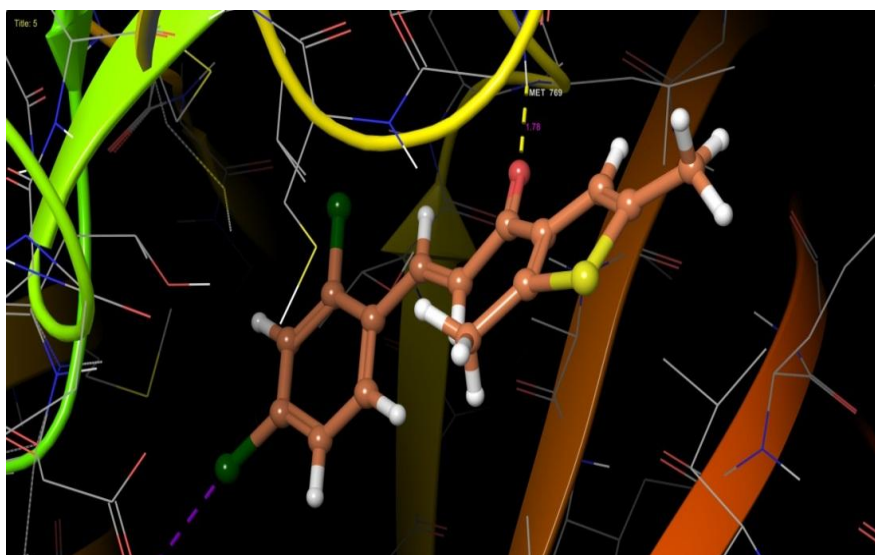


Fig. 2. 2D Representation of binding interactions of compound 5 with EGFR protein

Table 1. Predicted Molecular Properties of the Dataset Ligands and the Recommended Range of the Values

Molecule	MW	Dipole	SASA	FOSA	FISA	PISA	WPSA	Volume
1	287.333	0	552.239	173.871	140.735	196.812	40.821	932.148
2	256.362	0	546.313	262.067	43.469	199.956	40.821	919.523
3	260.326	0	523.104	173.84	43.463	217.938	87.863	875.638
4	276.78	0	520.147	166.584	42.863	232.154	78.545	883.435
5	311.225	0	544.183	166.581	42.861	184.542	150.2	927.581
6	278.316	0	513.281	169.832	43.497	198.516	101.436	874.46
7	258.334	0	526.547	173.901	98.002	213.823	40.822	882.323
8	321.778	0	558.297	166.659	140.084	172.984	78.57	955.957
9	301.359	0	576.633	247.503	127.801	160.514	40.815	985.72
10	332.414	0	620.19	411.096	43.499	124.781	40.814	1088.399
11	302.387	0	587.099	335.705	43.505	167.076	40.813	1014.77
12	321.231	0	543.106	173.841	43.463	207.647	118.155	912.521
13	243.323	0	507.845	174.228	71.544	221.254	40.819	846.802
14	322.424	0	621.196	228.538	56.899	294.975	40.785	1078.049
15	293.383	0	579.442	174.101	65.307	299.213	40.821	987.169
16	232.3	0	492.007	182.361	96.433	172.395	40.818	800.885
17	281.372	0	546.339	167.148	71.516	266.928	40.747	934.29
18	286.345	0	518.729	245.757	43.472	188.681	40.82	895.398
19	311.193	0	527.866	189.579	43.534	170.467	124.286	861.399
20	245.339	0	503.348	217.638	44.149	200.758	40.802	851.443

Recommended range: MW – molecular weight (130-725), dipole (1-12.5), SASA- solvent accessible surface area (300-1000), FOSA – hydrophobic component of SASA (0-750), FISA – hydrophilic component of SASA (7-330), PISA - π (carbon and attached hydrogen) component of the SASA (0.0 – 450.0), WPSA - Weakly polar component of the SASA (halogens, P, and S) (0.0 – 175.0), volume (500-2000)

Table 2. Predicted Pharmacokinetic (ADME) profiles of compounds

Molecule	CNS	QPlogPo/w	QPlogS	QPlogHERG	QPPCaco	QPlogBB	QPPMDCK	QPlogKp	QPlogKhsa	% Human Oral Absorption
1	-1	3.332	-4.021	-5.13	458.469	-0.981	356.355	-2.94	0.309	94.089
2	1	4.376	-5.049	-5.122	3834.317	0.009	3538.888	-1.232	0.583	100
3	1	4.028	-4.815	-5.06	3834.785	0.133	6406.464	-1.169	0.455	100
4	1	4.14	-4.718	-4.969	3885.355	0.125	5777.309	-1.108	0.478	100
5	1	4.865	-5.486	-4.916	3885.516	0.291	10000	-1.275	0.606	100
6	1	4.255	-4.688	-4.718	3831.951	0.181	7596.729	-1.238	0.452	100
7	0	3.37	-4.24	-5.061	1165.601	-0.553	977.018	-2.092	0.273	100
8	-1	3.604	-4.755	-4.936	465.035	-0.867	582.569	-3.012	0.378	95.788
9	-1	3.724	-4.938	-5.037	608.084	-0.872	483.531	-2.829	0.465	100
10	0	4.327	-4.783	-4.957	3831.776	-0.184	3536.033	-1.21	0.344	100
11	0	4.261	-4.711	-5.05	3831.264	-0.117	3535.49	-1.157	0.373	100
12	1	4.668	-5.326	-5.148	3834.798	0.2	9387.755	-1.205	0.562	100
13	0	3.043	-3.535	-4.976	2077.071	-0.234	1824.245	-1.675	-0.03	100
14	0	4.975	-5.945	-5.875	2859.768	-0.144	2576.377	-1.145	0.775	100
15	0	4.329	-5.154	-5.751	2380.091	-0.213	2113.589	-1.285	0.511	100
16	0	2.413	-3.384	-4.819	1206.213	-0.472	1013.821	-2.305	-0.129	96.225
17	0	4.252	-5.014	-5.297	2078.333	-0.244	1823.781	-1.513	0.599	100
18	1	3.508	-3.741	-4.598	3834.001	0.036	3538.509	-1.272	0.111	100
19	1	3.805	-4.802	-5.105	3828.856	0.206	10000	-1.337	0.28	100
20	1	3.4	-4.235	-4.704	3777.733	0.027	3481.646	-1.242	0.385	100

Recommended range: CNS Predicted central nervous system activity on a -2 (inactive) to +2 (active) scale; QPlogPo/w: Predicted octanol/water partition coefficient (-2.0 - 6.5); QPlogS: Predicted aqueous solubility (-6.5 - 0.5); QPlogHERG: Predicted IC50 value for blockage of HERG K⁺ channels (below -5); QPPCaco: Predicted apparent Caco-2 cell permeability in nm/sec. Caco-2 cells are a model for the gut-blood barrier (<25: poor, >500: great); QPlogBB: Predicted brain/blood partition coefficient (-3 - 1.2); QPPMDCK: Predicted apparent MDCK cell permeability in nm/sec. MDCK cells are considered to be a good mimic for the blood-brain barrier (<25: poor, >500: great); QPlogKp: Predicted skin permeability, log Kp (-8.0 - -1.0); QPlogKhsa: Prediction of binding to human serum albumin (-1.5 - 1.5); %Human- Oral Absorption (>80% is high, <25% is poor)

Table 3. Docking results and protein-ligand binding interactions of anti-bacterial, anti-fungal chalcone derivatives with EGFR protein

COMPOUND	DOCK SCORE	NO OF H-BONDS	INTERACTING AMINO ACIDS	H-BOND DISTANCE (Å)	Binding energy
1	-5.764	1	MET 769	2.07	-32.262
2	-6.075	1	MET 769	2.02	-33.463
3	-5.681	1	MET 769	2.13	-30.988
4	-6.259	1	MET 769	2.10	-34.078
5	-6.746	1	MET 769	1.78	-34.578
6	-6.423	1	MET 769	1.94	-31.597
7	-6.622	2	MET 769	1.99	-38.845
			ASP 831	1.94	
8	-6.173	2	MET 769	1.73	-29.58
			LYS 721	2.03	
9	-6.278	2	MET 769	1.78	-35.642
			LYS 721	2.00	
10	-6.498	2	MET 769	2.09	-38.367
			LYS 721	2.08	
11	-6.516	2	MET 769	2.08	-35.855
			LYS 721	2.06	
12	-6.125	1	MET 769	1.95	-33.842
13	-6.06	1	MET 769	1.79	-26.912
14	-6.417	2	MET 769	2.30	-32.776
			THR 830	2.34	
15	-6.535	1	MET 769	1.77	-33.855
16	-5.99	1	MET 769	2.08	-31.644
17	-6.32	1	MET 769	1.91	-33.257
18	-6.368	1	MET 769	1.96	-37.22
19	-6.177	1	MET 769	2.09	-31.424
20	-6.359	0	-	-	-27.522

4. CONCLUSION

In the current investigation, we have hypothesized the probable EGFR inhibitory potentials of anti-bacterial, antifungal chalcone derivatives, and docking simulations were performed to identify binding efficiency and binding energy towards the EGFR protein. Among all the tested dataset ligands, compound 5 has shown the highest dock score (-6.746) with better ADME profiles. Binding energies in the protein-ligand interactions explain how fit the ligand binds with the target protein. Molecular docking studies of these anti-bacterial, antifungal chalcone derivatives provided deeper insights in understanding the probable conformations of these tested ligands in the EGFR protein environment.

ACKNOWLEDGEMENTS

The authors would like to thank Sarojini Naidu Vanitha Pharmacy Maha Vidyalaya, Tarnaka, Secunderabad-17, Telangana and its Management for providing facilities for the

research work. The authors are thankful for the support given by Mrs. Siva Jyothi Buggana, Dept. of Pharmaceutical Chemistry, Bojjam Narasimhulu Pharmacy College for women, Saidabad, Hyderabad.

CONSENT

It is not applicable.

ETHICAL APPROVAL

It is not applicable.

COMPETING INTERESTS

Authors have declared that no competing interests exist.

REFERENCES

1. Vishwanadham Yerragunta, et al. a review on chalcones and its importance, PharmaTutor Magazine. 2013;1(2):54-59.

2. Hemalatha sattu et al., Synthesis, biological activity and molecular properties prediction of novel chalcones, Indian Journal of Heterocyclic Chemistry. 2014; 23:367-376.
3. Go ML, Wu X, Liu XL. Chalcones an Update on Cytotoxic and Chemo protective Properties Curr. Med. Chem. 2005;12:483-499.
4. Ballesteros, J. F et al., An efficient green procedure for the synthesis of chalcones, J. Med. Chem. 1995;38:2794.
5. Mukerjee VK, et al. A review on chalcones and its importance, Bioorg. Med. Chem. 2001;9:337.
6. Sivakumar PM, Geetha Babu SK, Mukesh D. QSAR Studies on Chalcones and Flavonoids as Anti-tuberculosis Agents Using Genetic Function Approximation (GFA) Method, Chem. Pharm. Bull. 2007; 55:44-49.
7. Liu UM, et al. Structure-activity relationships of antileishmanial and antimalarial chalcones, Bioorg. Med. Chem. 2003;11:2729-2738.
8. Viana GS, Bandeira MA, Mantos FJ. Analgesic and antiinflammatory effects of chalcones isolated from Myracrodruon urundeuva allemão, Phytomedicine. 2003; 10:189.
9. Tiwari N, et al. Novel 2'-amino chalcones: design, synthesis and biological evaluation, Bioorg. Med. Chem. 2000;10: 699.
10. Ducki S, et al. Potent antimitotic and cell growth inhibitory properties of substituted chalcones, Bioorg. Med. Chem. 1998;8: 1051.
11. Krystof V, et al. 4-arylazo-3,5-diamino-1H-pyrazole CDK inhibitors: SAR study, crystal structure in complex with CDK2, selectivity, and cellular, J. Med. Chem, 2006;49(22):6500-6509.
12. Harathi P, et al. synthesis, characterization and anti-inflammatory activity of novel Pyrazole derivatives, Asian J. Pharm. Clin. Res. 2015;8:83-87.
13. Ligprep, Version 2.7, Schrodinger LLC, NY, USA; 2016.
14. Gade DR, et al. Structural insights of JAK2 inhibitors: pharmacophore modeling and ligand-based 3D-QSAR studies of pyrido-indole derivatives, J. Recept. Sig. Transd. 2014;35(2):189-201.
15. Reddy GD, et al. ADMET, Docking studies & binding energy calculations of some Novel ACE-inhibitors for the treatment of Diabetic Nephropathy, Int. J. Drug Dev. Res. 2012;4(3):268-282.
16. Chaitanya P, et al. Design and Synthesis of Quinazolinone Derivatives as Anti-inflammatory Agents: Pharmacophore Modeling and 3D QSAR Studies, Med. Chem. 2014;10(7):711-723.
17. Siva Jyothi B, et al. Novel 2,4-disubstituted quinazolines as cytotoxic agents and JAK2 inhibitors: Synthesis, in vitro evaluation and molecular dynamics studies, Comput. Biol. Chem, 2019;79: 110-118.

© 2021 Sattu et al.; This is an Open Access article distributed under the terms of the Creative Commons Attribution License (<http://creativecommons.org/licenses/by/4.0>), which permits unrestricted use, distribution, and reproduction in any medium, provided the original work is properly cited.

Peer-review history:
The peer review history for this paper can be accessed here:
<https://www.sdiarticle4.com/review-history/74657>